

SUPPORTING INFORMATION FOR:

David Muñoz-Rojas,* Judith Oró-Solé, Pedro Gómez-Romero,* **Spontaneous Self-Assembly of Cu₂O@PPy nanowires and anisotropic crystals.**

davidmunozrojas@gmail.com, pedro.gomez@cin2.es

EXPERIMENTAL DETAILS:

Synthesis: Pyrrole (98%, Aldrich) was vacuum-distilled and stored under argon at -4 °C prior to its use. CuO (97%, Aldrich) was used as received. In a typical reaction, 140 µl (2 mmol) of pyrrole (Py) were dissolved in 20 mL of distilled water and CuO was added to the solution. The mixture was stirred for different times, and the suspension obtained was transferred to a 25 mL screw-capped Pyrex bottle. The bottle was then tightly closed with a Teflon cap and heated at different temperatures for various times. After reaction the samples were filtered off, washed with distilled water, and dried at 50 °C. The particular conditions for each reaction are listed in Table S1. For the experiments carried out with ground CuO, the commercial powder was treated in a ball mill for 4 h.

Characterization: Transmission electron microscopy (TEM) images and selected area electron diffraction (SAED) patterns were obtained on a JEOL 1210 transmission electron microscope operating at 120 kV and equipped with a side-entry (60°/30°) double tilt. High-resolution images were obtained with a JEOL JEM 2011 electron microscope (Serveis Científicotècnics, Autonomous University of Barcelona) operating at 200 kV. In all cases TEM samples were prepared by dispersing powders of the sample in absolute ethanol. Carbon-coated copper grids were used. Scanning electron microscopy (SEM) images were obtained with a FEI Quanta 200 F field-emission gun (FEG) electron microscope and a Hitachi S-570 (Serveis Científicotècnics, Autonomous University of Barcelona). X Ray diffraction of the powders was performed with a rotating anode Rigaku Rotaflex Ru-200B diffractometer with CuK α radiation ($\lambda_1 = 1.5060 \text{ \AA}$ and $\lambda_2 = 1.5444 \text{ \AA}$) in the angular range $5 \leq 2\theta \leq 75^\circ$, with a step size of 0.02° and at a scanning rate of $0.16^\circ \cdot \text{min}^{-1}$.

Table S1: Summary of several reactions carried out in different conditions.

R. #	CuSO ₄ / mg(mmol)	Py / μ l(mmol)	Temp. / °C	Time / h	Phases in XRD patterns
1	328.0 (2.06)	140 (2.02)	120	22.4	Cu
2	304.3 (1.91)	140 (2.02)	150	41	Cu
R. #	CuO / mg	Py / μ l	Temp. / °C	Time / h	Phases in XRD patterns
3	166.5 (2.09)	140 (2.02)	120	22.4	CuO
4	164.2 (2.06)	140 (2.02)	150	24	CuO, Cu ₂ O
5	163.9 (2.06)	140 (2.02)	150	72	CuO, Cu ₂ O
6	164.7 (2.07) ; Manually ground	140 (2.02)	150	24	Cu ₂ O, CuO
7	168.0 (2.11) ; Manually ground	280 (4.04)	150	24	Cu ₂ O, CuO
8	104.0 (1.31) ; Milled	140 (2.02)	150	21	Cu ₂ O, CuO
9	102.2 (1.28) ; Milled + stirred 5d	140 (2.02)	150	24.5	Cu ₂ O, (CuO)
10	102.1 (1.28) ; Milled	140 (2.02)	150	29	Cu ₂ O, CuO
11	102.2 (1.28) ; Milled	140 (2.02)	150	96	Cu ₂ O
12	115.0 (1.44) ; Milled	140 (2.02)	165	64.5	(CuO), Cu ₂ O, (Cu)

The effect of the different Cu²⁺(aq) reduction potential as compared to CuO can be observed when comparing reactions 1 with 3, and 2 with 5: while large Cu⁰ particles are obtained (see Fig. S1) when using a Cu²⁺ soluble precursor (CuSO₄) at both 120 and 150 °C, commercial CuO does not react at 120 °C, and does only partially at 150 °C after 72 h.

The surface-limiting nature of the reaction is supported by several facts: i) smaller CuO particle sizes lead to faster reaction. (Compare reactions 4 & 6). ii) longer stirring periods before the hydrothermal treatment had the same effect due to a decrease in the initial particle sizes (compare reaction 8 or 10 with 9). iii) On the contrary, increasing the amount of Py above that of the optimized experimental procedure does not lead to a faster reaction (compare 6 & 7). Finally, temperature also plays an important role in the outcome of the reduction, though not in the morphology of the products. Thus, when the reaction was carried out at 120 °C, no reduction took place after 24 h (r. 3). On the other hand a reaction using ground CuO at 165 °C for 64 h led to a reduction beyond Cu(I), yielding Cu₂O and Cu⁰, together with some unreacted CuO (r. 12). After 4 days only Cu₂O and Cu⁰ were present. Conversely, Cu₂O was the only reduction product when using milled CuO at 150 °C for 96 h (r. 11).

Figure S1: SEM images of two different samples synthesized using Cu^{2+} (CuSO_4) instead of a CuO suspension. A: crystals obtained for the reaction 1 in Table S1; B: crystals obtained for the reaction 2 in Table S1. Image acquired with secondary electrons; C: Same crystal as in B, acquired using backscattered electrons to enhance the differentiation between PPy and metallic Cu.

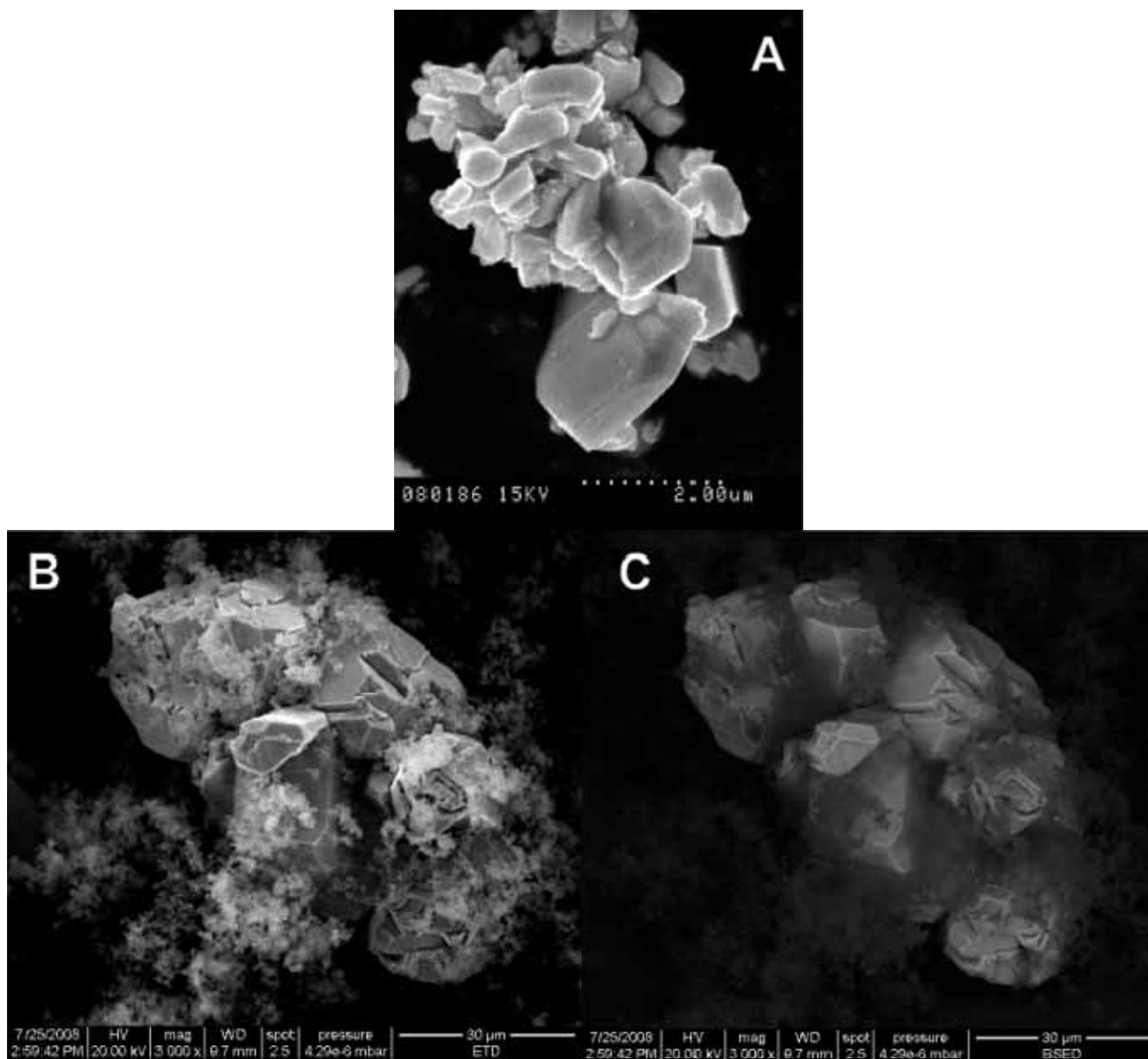


Figure S2: SEM images of commercial CuO (A & B) and after ball milling it for 4 h (C & D).

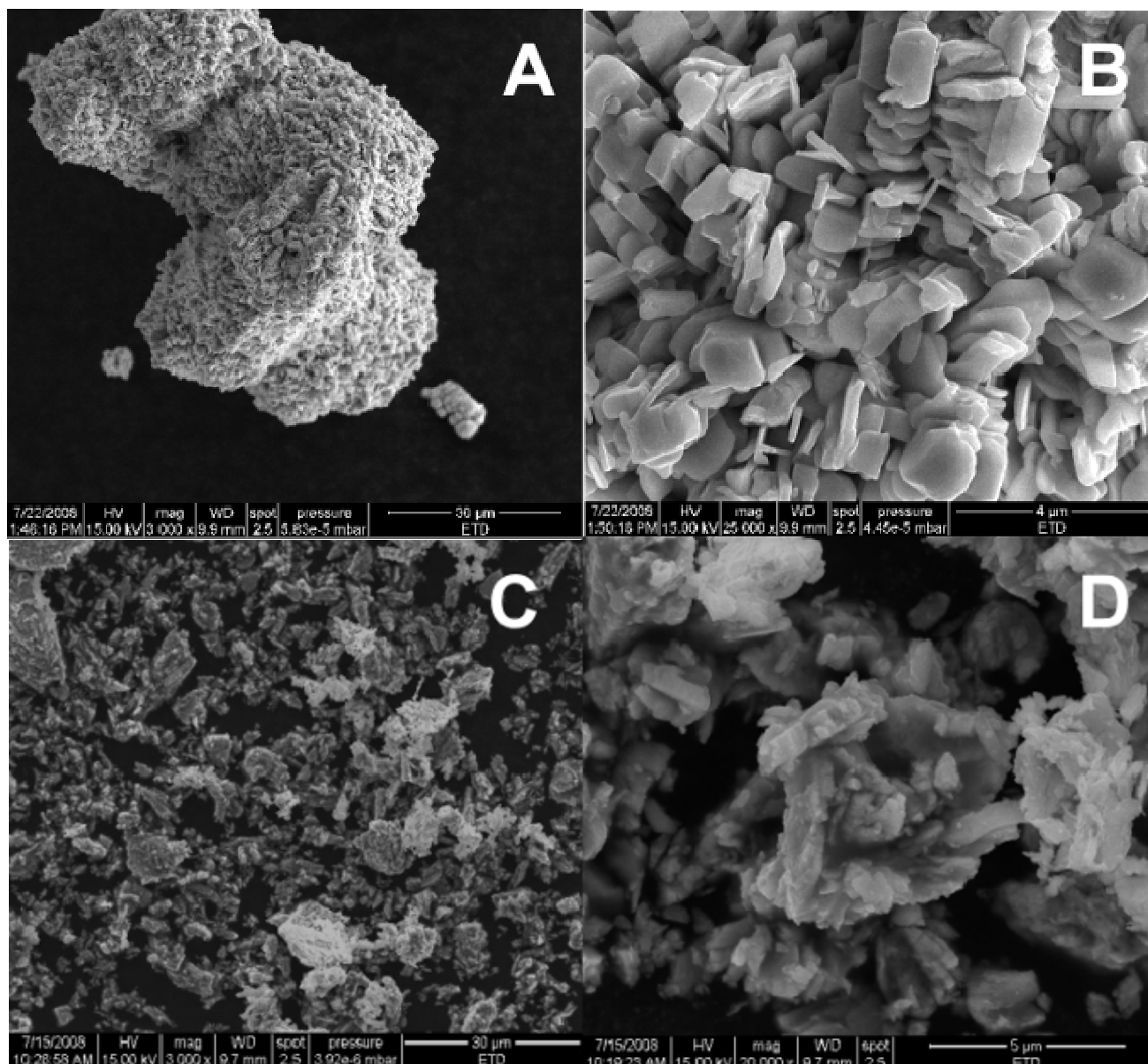


Figure S3: Larger version of the HRTEM image appearing in the Inset 2 in figure 1b in the text. The simulated SAED, as well as the lattice fringes, clearly show a perfect crystallographic matching. The spacing indicated corresponds to the Cu_2O {111} planes. This type of particles gives rise to the characteristic surface roughness observed in some wires.

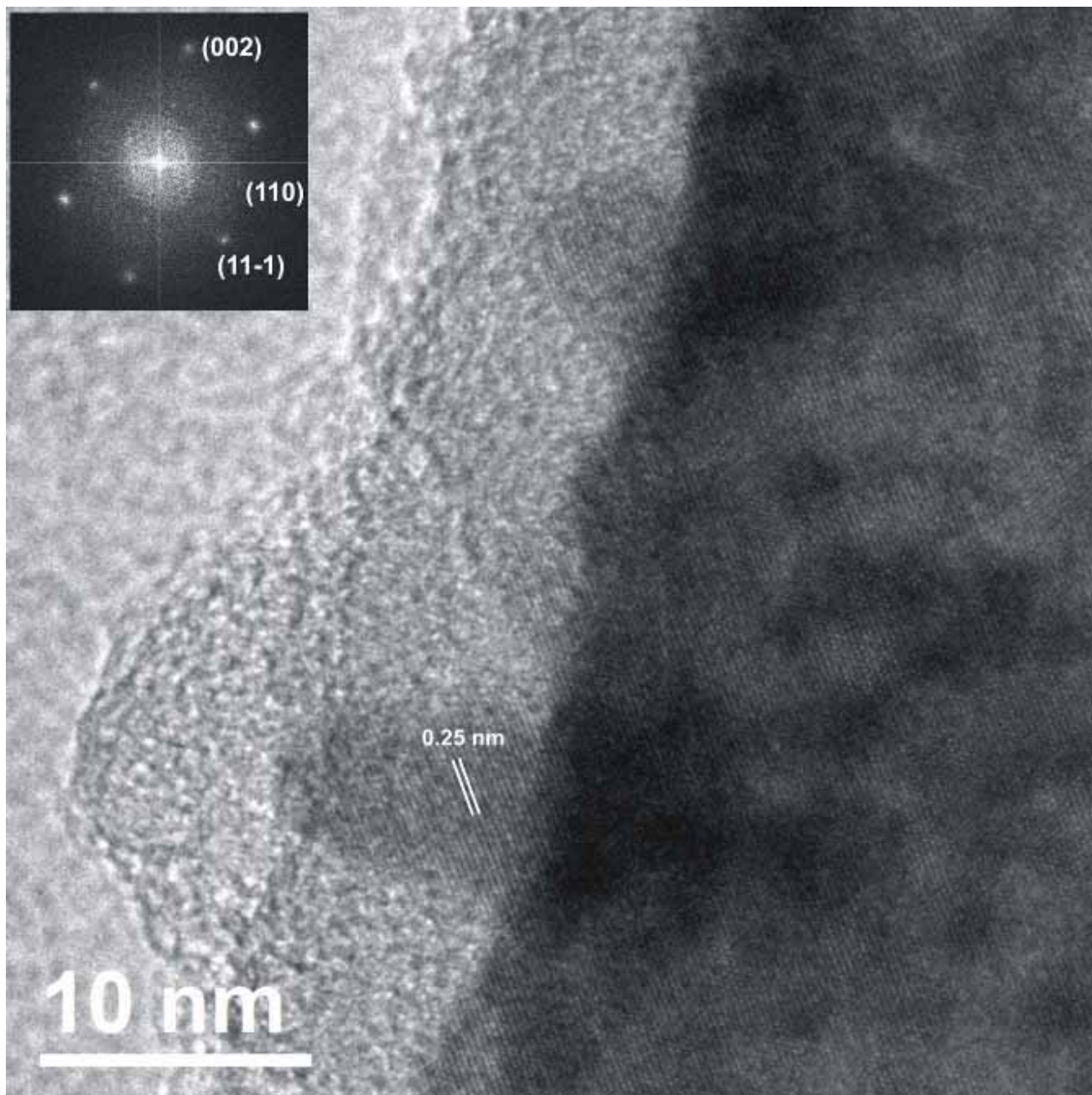


Figure S4: HRTEM images of several nanowires in which lattice matching can be observed. The arrow indicates the longitudinal axis of the main wire, and corresponds to the $\langle 001 \rangle$ direction.

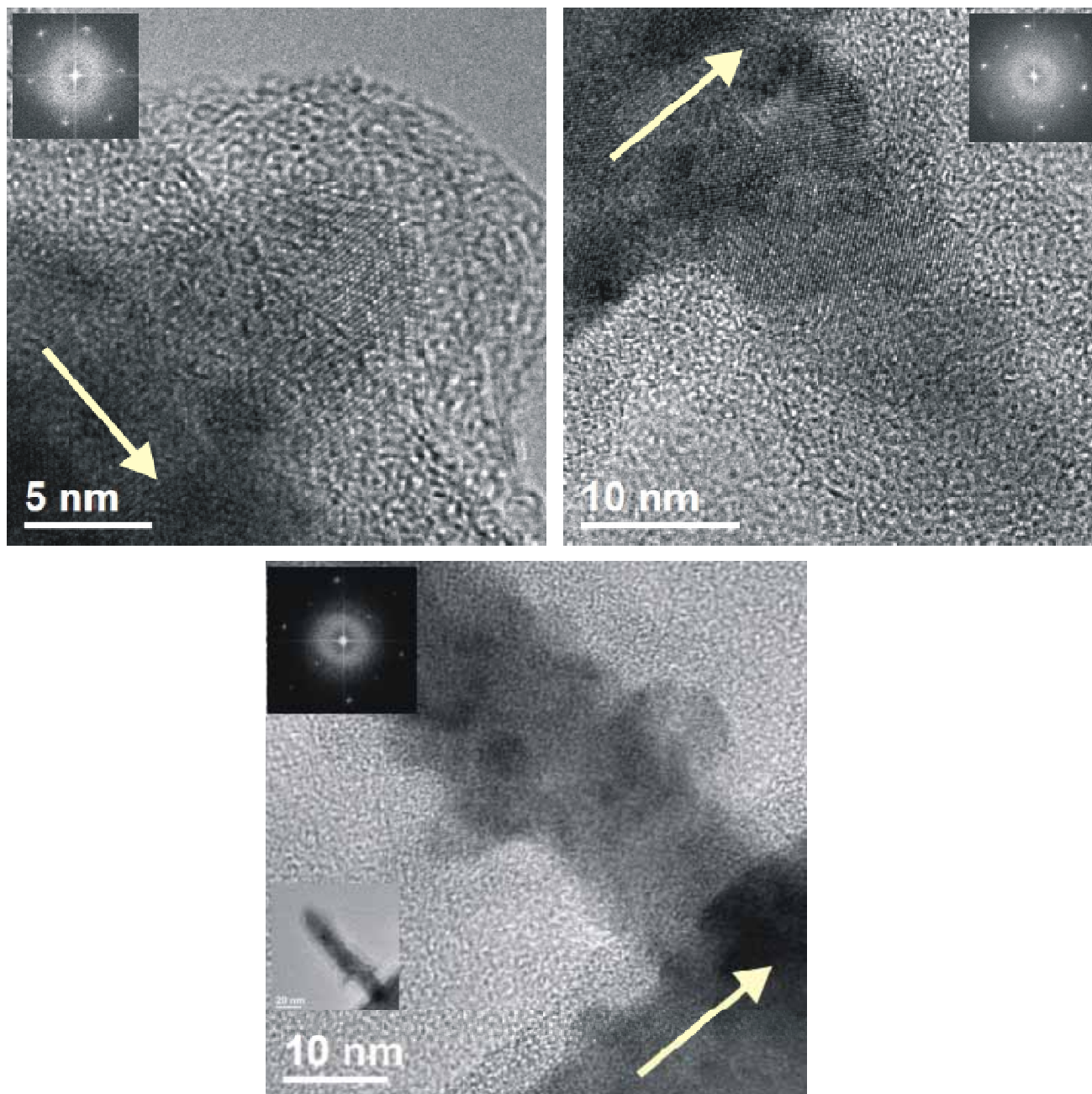


Figure S5: TEM images and X ray patterns of the products obtained for increasing reaction times: After 30 min of reaction at 150 °C no nanowires had formed, having only the initial CuO particles of different sizes. After 1h, PPy spheres were already appreciated but not wires. After 2,5 h, the first thin nanowires appeared. With increasing reaction time, a qualitative increase of the number of nanowires as well as of its diameters is clearly observed. For reaction periods as short as 6 h, more complex, branched structures can be already found. After 42 h and longer times, thicker nanowires and branched structures are accompanied by bigger crystals. After 8 days of reaction, Cu peaks were present in the diffraction pattern.

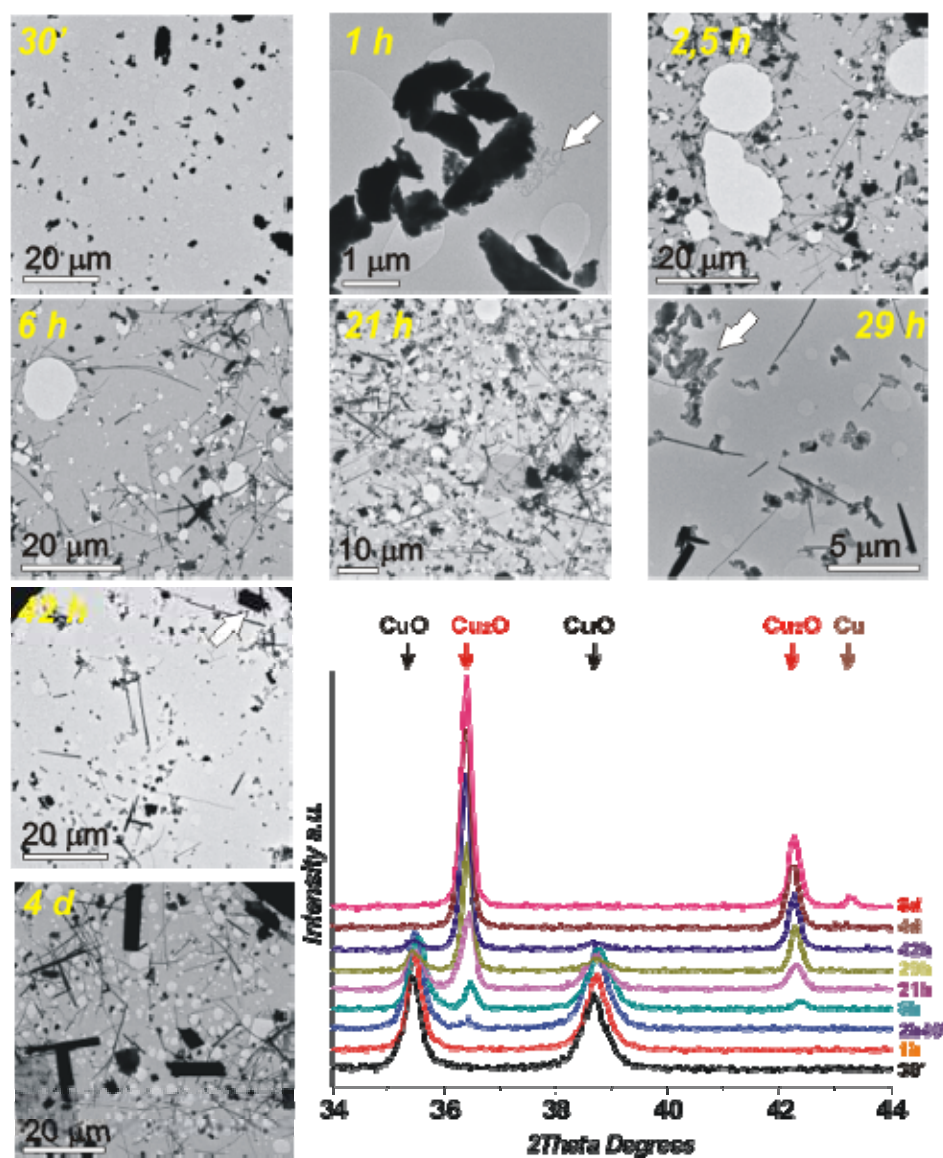


Figure S6: TEM image of a Branched $\text{Cu}_2\text{O}@PPy$ nanostructure. Several SAED patterns taken from different positions are identical, thus showing that the branched structure is a single crystal.

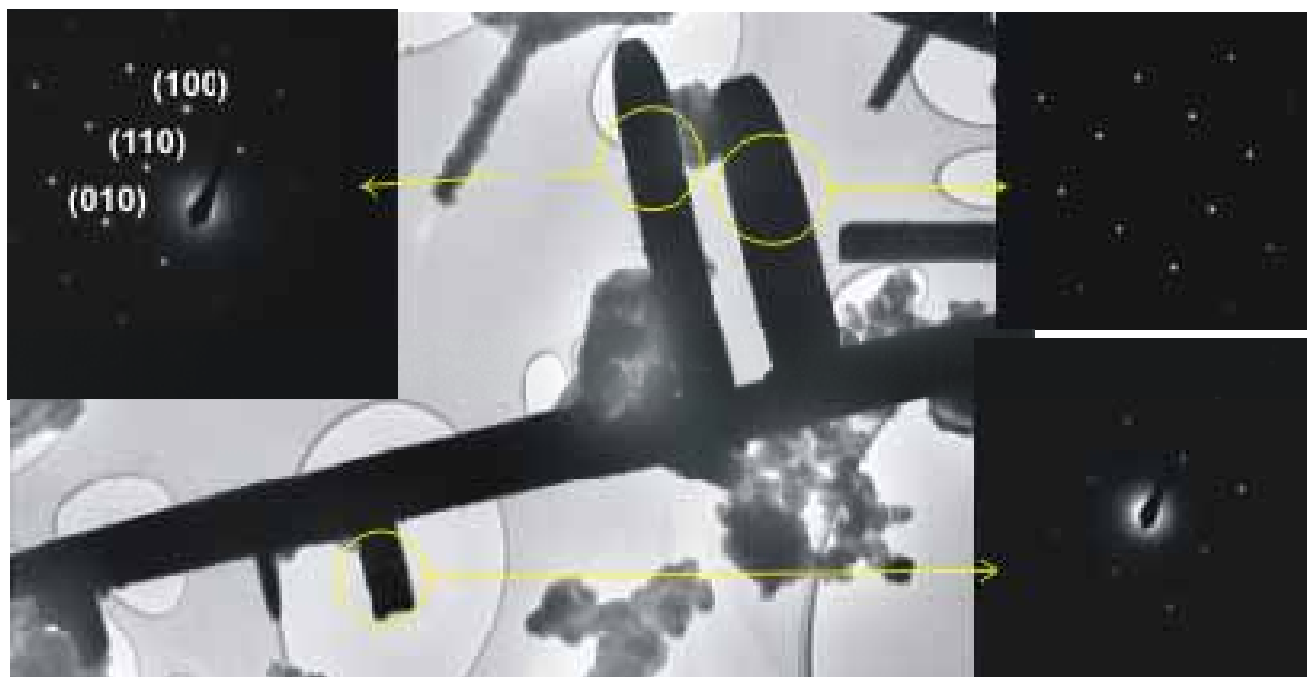


Figure S7: TEM images of Cu₂O@PPy core/shell branched structures before (A & B) and after (A' & B') prolonged exposure to an intense electron beam.

